FAST FLOW BURSTS AND AURORAL ACTIVATIONS

R. Nakamura[1], W. Baumjohann[1], V. A. Sergeev[2], M. Kubyshkina[2], M. Brittnacher[3], G. Parks[3], K. Liou[4], T. Mukai[5]

[1]Max-Planck-Institut für extraterrestrische Physik, D-85740 Garching, Germany
(Tel: +49-89-3299-3325, Fax: -3569; e-mail: rumi@mpe.mpg.de)
[2]Geophysics Program, University of Washington, Seattle, Washington 98195, USA
[3]Institute of Physics, St. Petersburg University, St. Petersburg 198904, Russia
[4]Institute of Space and Astronautical Science, Sagamihara, Kanagawa, Japan
[5]Applied Physics Laboratory, Laurel, 20723 MD, USA

ABSTRACT

Flow burst events with a dawn-to-dusk electric field exceeding 2 mV/m and with a duration of less than 10 min observed by Geotail are compared with auroral data from the Polar ultraviolet imager. Temporal and spatial relationships between the flow bursts and the aurora are examined. It is shown that all the flow bursts correspond either to a localized auroral intensification associated with small poleward expansions and pseudobreakups or to activations starting at poleward edge of the expanded auroral oval, including auroral streamers, that develop equatorward toward the foot point of the satellite. Although most of these auroral activations precede the flow bursts by a few minutes, the activations that break up near the foot point of the satellite start within ± 1 min of the flow burst onset.

1 INTRODUCTION

Determining the timing of fast flows relative to substorm phase and location of initial brightening and current wedge is essential to test the different substorm models. It is difficult, however, to identify this relationship by merely using the distance from the Earth or from the timing relative to the onset of the auroral electrojet indices, since each substorm intensification takes place in a limited local time region and at different locations. Simultaneous global auroral images, which include both temporal and spatial information, are therefore crucial to determine spatial/temporal relationships between the flows and auroral disturbances.

Several different types of auroral activation are observed during fast Earthward flow events in the tail between $X = -10R_E$ and $X = -30R_E$. Fairfield et al. (1999) reported local brightening and expansion of aurora that developed near the foot point of the satellite. Sergeev et al. (1999) reported auroral streamers (N-S aurora) that suggested a flow channel in the magnetosphere at the foot point of the satellite. Activation and equatorward expansion of high-latitude auroral patches toward the foot point of the satellite have also been observed (Nakamura et al., 1998; Sergeev et al., 2000).

In this study we statistically examine the temporal and spatial relationships between fast flow bursts and auroral activations in the same local time sector. Data from the Geotail magnetic field (MGF; Kokubun et al., 1994) and low energy particle (LEP; Mukai et al., 1994) experiments are analyzed and compared with auroral data obtained from the Polar UVI experiment (Torr et al., 1995).

2 FLOW BURSTS AND ASSOCIATED AURORAL SIGNATURES

We select Geotail flow bursts events between April 1996 and December 1997 using the following criteria: flows with strong convection electric field ($|(V_X \times B_Z)| > 2$ mV/m) in the inner plasma sheet ($\beta > 0.5$) and when the satellite was located near midnight ($-30R_E < X_{GSM} < -10R_E, -5R_E < Y_{GSM} < 5R_E$). Here, enhancements in the electric field which are not separated by more than 5 min are regarded as the same electric field enhancement event. We concentrate on events with a total duration not exceeding 10 min. To examine what type of aurora activation take place in association with the flows, we surveyed all auroral images from the Polar UVI experiment for the flow burst events. There were 31 events in total when Polar UV images were available simultaneously

with the flow observations. 27 events correspond to Earthward flow, while 4 events show tailward flows.

All 31 flow burst events correspond to some auroral activation. The types of aurora observed associated with the flows can be divided into three categories: aurora related to poleward expansion/pseudobreakups, 13 events; N-S aurora (auroral streamer), 11 events; high-latitude activation (auroral patch or activation of a surge), 7 events. Whereas the first type of aurora is related to the expansion phase of a small substorm or pseudobreakup, the latter two are related to an activation later in the expansion or recovery phase preceded by poleward expansion of aurora.

Figure 1 shows a Polar UVI image from 2117:48 UT on December 10, 1996, during an auroral streamer (or N-S aurora), which extends equatorward from high latitudes (78°). On December 10, 1996, a major substorm broke out at 1659 UT, with two major poleward expansions and the auroral oval was expanded up to (82°) and followed by multiple activations of the high-latitude patches and periods of equatorward extending auroral streamers (not shown). These auroral activations, which took place during enhanced convection as indicated in the ground magnetograms, were accompanied by fast flow bursts until 22 UT. General relationships between these auroral activations and the flow bursts are given by Nakamura et al. (1998) and Sergeev et al. (2000) and an analysis of an auroral streamer compared with fast flow and velocity dispersed ions observations is given by Sergeev et al. (1999). The auroral streamer shown in Figure 1 is observed near the end of the enhanced convection period.

Shown in Figure 1 is also the Geotail foot point, calculated from two different models: the circle shows the foot point calculated using the Tsyganenko 89 (T89) model [*Tsyganenko, 1989*] for $Kp = 4$, which fits best to the Geotail observations for this instance; the cross shows the foot point calculated using the Hybrid Input Algorithm (HIA) model [*Kyubishkina et al., 1999*]. The latter model uses input from several spacecraft measurements to modify the tail current and ring current of the T89 model in order to obtain a best fit to the satellite observations so that more accurate mapping can be performed. For this particular event, ring currents are weakened to 63% of the T89 model level and the tail current was tilted 2.5° to obtain best fit to the Geotail data and symmetric axis of the particle distribution in Los Alamos Satellite data. The foot point calculated using the HIA model is located just south-east of the auroral streamer, while the foot point of the T89 model is located much further south. The first signature of the equatorward extension of this slanted N-S aurora (auroral streamer) was apparent in the 2115:11 UT image (not shown) extending equatorward from 75° latitude. The aurora extended equatorward as can be seen in 2117:48 UT image. The auroral streamer decayed by

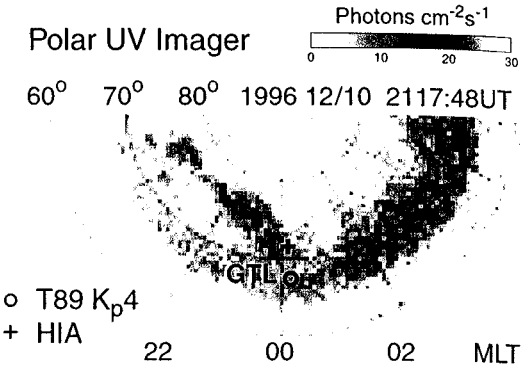

Figure 1. UVI image from 2117:48 UT on December 10, 1996, shown in geomagnetic coordinates. The foot point of Geotail is marked in the figure using two different magnetic field models as described in the text.

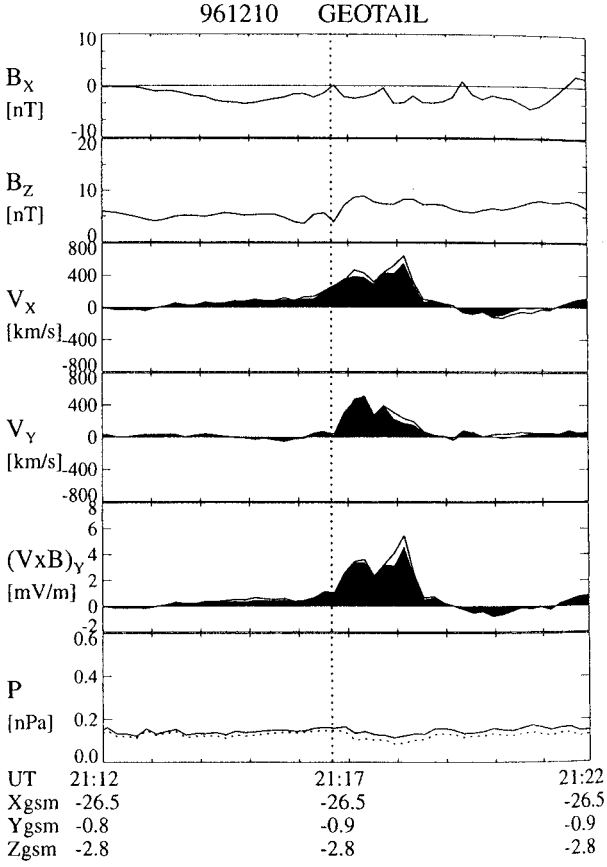

Figure 2. Magnetic field and plasma signatures detected by Geotail on December 10, 1996. Shown are B_X, B_Z, V_X, V_Y, Y-component of the $-V \times B$ electric field, and pressure. Contribution from the flow component perpendicular to the ambient magnetic field is shown as black area in the plots of V_X and V_Y. The black area in the fifth panel shows the contribution from $V_X \times B_Z$. While the solid line shows the total pressure, the broken line shows the plasma pressure. The vertical line indicates the onset time of the flow burst event.

2120:52UT.

Magnetic field and plasma signatures detected at Geotail

during the period of the auroral streamers are shown in Figure 2. Geotail was located in the plasma sheet (see the high contribution of the plasma pressure to the total pressure in Figure 2a) at $X_{GSM} = -26.5R_E$ near midnight, and observed fast Earthward and duskward flow associated with a change toward a dipolar configuration. The flow was directed mainly perpendicular to the magnetic field. The dawn-to-dusk electric field, $-(V \times B)_Y$, reaches 6 mV/m during the flow events and is mainly contributed by $V_X \times B_Z$. The onset of the fast flow was at 2116:40 UT, which corresponds to the time when the aurora was expanding toward the Geotail location.

To examine the spatial relationship between flow and auroral signature, we determined the relative location of the localized plasma structure using the method used by Sergeev et al. (1996), in which the shear structure at the front side of the fast flowing plasma is analyzed to determine the relative location of the high-speed flowing plasma-depleted flux tubes, or "bubbles", based on the model of Chen and Wolf (1993). Sergeev et al. (1996) showed that the Earthward moving plasma structures are separated from the plasma ahead of them by a sharp discontinuity. It is then expected that the layer ahead of the plasma structures exhibits flow and magnetic field shear consistent with flow around a moving obstacle. For example, in the case of an Earthward moving plasma structure that is located duskside (dawnside) of the observation point, the front layer's normal direction should be tilted dawnward (duskward) and should observe a dawnward (duskward) directed flow component. In this way, it can be checked from the front-side shear of the flow and the change in the direction of the magnetic field, whether the structure is located at the duskside or the dawnside of the observation point. Since the flows must not always be directed exactly Earthward, even if observed at the center of the flow, we checked whether the rotation of the flow in the X-Y plane is clockwise (anti-clockwise) viewed from the north to identify whether the flows is observed at the duskside (dawnside) of the satellite, instead of using the dawn-dusk component of the flow.

For this event we identified the front layer to be centered at 2116:40 UT. From the minimum variance analysis of the magnetic field data between 2116:07 and 2117:31 we obtained a negative Y-component of the normal direction of the layer, and a clockwise rotation of the plasma flow across the layer, which indicates that the plasma structure is located duskward of the satellite. This coincides with the location of the auroral streamer, which is also located duskward of the satellite's foot point as shown in Figure 1. In this example, the plasma flows are therefore very likely associated with the auroral streamer, which is an equatorward stretching auroral structure. The timing of the auroral feature suggests that the aurora started to evolve first at high latitudes, corresponding to a source mechanism operating tailward of the satellite, and then extends equatorward where the Geotail foot point is located.

3 TIMING OF FLOWS AND AURORAL ACTIVATION

Timing and location (latitude and MLT) of the aurora relative to that of the flow bursts are plotted in Figure 3 for different types of aurora (the asterisks correspond to pseudobreakup/small expansion, the diamonds to auroral streamer, and the triangles to high-latitude activation). Here the location of the aurora is examined with a resolution of 1° in latitude and 0.25 MLT.

The left three plots show the location of the auroral brightening for the relative onset time, t_0. The top plot shows the latitude distribution obtained by using the T89 model, the middle plot shows the latitude obtained by using the HIA model, and the bottom plot shows the MLT obtained by using the HIA model. $t_0 \equiv t_{a0} - t_{f0}$, where t_{a0} is the onset of the auroral activation and t_{f0} is the onset of the flow. t_{a0} is obtained by examining the auroral images to identify the onset of the activation. The midtime between the time of the last image without aurora and the first image with aurora is plotted as symbol in the figure, and the ends of the error bars present the times of these two images. t_{f0} is defined as the onset time of electric field enhancement, $V_X \times B_Z$. Most of the auroral activations precede the flow enhancements as can be seen in the left-hand side plots. This tendency is particularly clear for those related to higher latitude auroral activations, such as N-S aurora and high-latitude patches. For cases when the auroral activation starts near the latitude of Geotail foot point the auroral types were exclusively the pseudobreakup/expansion type aurora. Although, both the T89 and HIA models show this tendency, the foot points are predicted to be closer to the auroral brightening region, particularly when the flow events occur within 5 min of the auroral brightening. The bottom left plot shows that the auroral activation starts at the same local time or earlier local time of the foot point. The aurora precede the flow activations by 2.9±3.0 min on average. Particularly, in those cases when the latitude of the breakup region is several degrees higher or 1 MLT earlier, the time difference becomes large. On the other hand, the auroral activations that break up near the foot point of the satellite start within ±1 min of the flow burst onset.

The right three plots show the location of the aurora for the maximum of the events, t_{MAX}, for latitude (top and middle plots) and MLT (bottom plot). $t_{MAX} \equiv t_{aM} - t_{fM}$, where t_{aM} is the time when most intense aurora was detected in Polar UV image and t_{fM} is the time of the maximum in the flow (electric field), t_{fM}. The symbols correspond to the onset region while the bars present the maximum extent of the aurora. Most of the bars cross

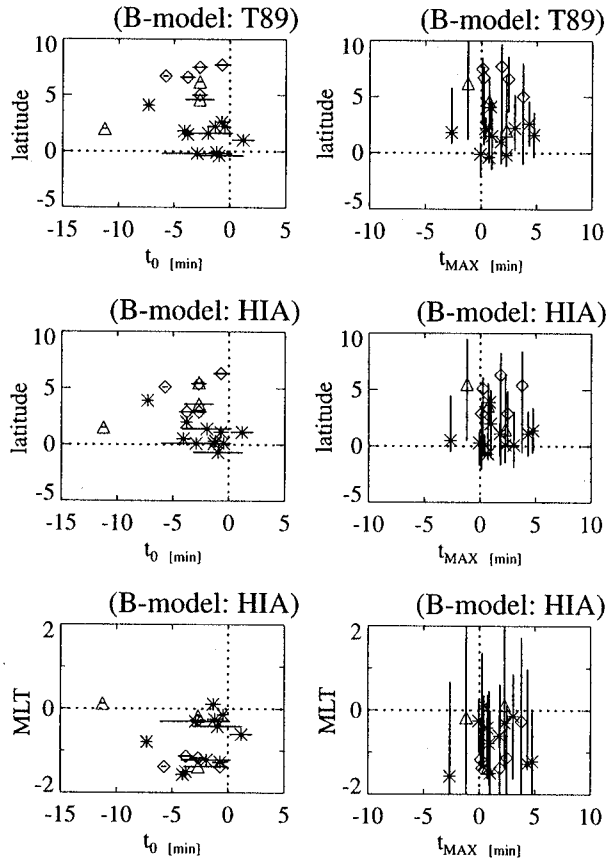

Figure 3. Timing and location (latitude and MLT) of the aurora relative to that of the flow bursts for different types of aurora: the asterisks correspond to pseudobreakup/small expansions, the diamonds to auroral streamers, and the triangle to other high-latitude activations. The left three plots show the location of the auroral brightening for the relative onset time, while the right three plots show the location of the aurora for the maximum of the events.

the zero level in latitude and MLT, which indicate that these auroral activations reach the Geotail foot point location in the course of development. The right top and middle plots show that the aurora extend closer to the foot point latitude for the HIA model as compared to the T89 model, and therefore the former model predicts a closer relationships between aurora and flows. The timing of the maximum of the expansion of aurora is slightly preceded by the maximum of the flows (1.4±1.8 min), which indicates that the flow event maximize while the aurora is still developing. Hence close relationships are obtained both temporal and spatial between the aurora and the flow bursts.

4 SUMMARY AND CONCLUSIONS

We examined the temporal and spatial relationships between the flow bursts and the auroral activation near the satellite foot point. The flow bursts correspond to different auroral types: poleward expansion, pseudobreakup, auroral streamer (N-S aurora), and high-latitude activation. The frontside flow shear of the fast flow is shown to be consistent with strong cross-tail localization of flow bursts. Close relationships are obtained both temporal and spatial between the aurora and the flow bursts. Although most of the auroral activations precede the flows, the auroral activations that break up near the foot point of the satellite start within ±1 min of the flow burst onset. The time difference becomes large for those cases when the latitude of the breakup region is several degrees higher or 1 MLT earlier. The aurora expands covering locations of the satellite foot points.

ACKNOWLEDGMENTS

We thank S. Kokubun for Geotail MGF data. We thank T. Nagai, N. Sckopke and T. Bauer for helpful comments. We very much appreciate A. Allner and G. Leistner for their help with the data processing.

REFERENCES

Chen, C. X., Wolf, R. 1993, J. Geophys. Res., 98, 21409

Fairfield, D. H. et al. 1999, J. Geophys. Res., 104, 355

Kokubun, S. et al. 1994, J. Geomagn. Geoelectr., 46, 7

Kubyshkina, M. et al. 1999, J. Geophys. Res., 104, 24977

Mukai, T. et al. 1994, J. Geomagn. Geoelectr., 46, 669

Nakamura, R. et al. 1998, In: Kokubun, S., Kamide, Y. (eds.) SUBSTORMS-4, Terra Sci./Kluwer Acad., 179

Sergeev, V. A. et al. 1999, Geophys. Res. Lett., 26, 417

Sergeev, V. A. et al. 2000, Geophys. Res. Lett., 27, 851

Torr, M. R. et al. 1995, Space Sci. Rev., 71, 329

Tsyganenko, N. A. 1989, Planet. Space Sci., 37, 5